Hindawi
Advances in Civil Engineering
Volume 2018, Article ID 9827673, 11 pages
https://doi.org/10.1155/2018/9827673

Research Article

Numerical Modeling of Thermal-Dependent Creep Behavior of Soft Clays under One-Dimensional Condition

Qi-Yin Zhu and Ping Qi

State Key Laboratory for Geomechanics and Deep Underground Engineering, China University of Mining and Technology, Xuzhou 221008, China

Correspondence should be addressed to Qi-Yin Zhu; qiyin.zhu@gmail.com

Received 29 June 2018; Revised 20 September 2018; Accepted 25 September 2018; Published 17 October 2018

Academic Editor: Dingwen Zhang

Creep is a common phenomenon for soft clays. The paper focuses on investigating the influence of temperature on the time-dependent stress-strain evolution. For this purpose, the temperature-dependent creep behavior for the soft clay has been investigated based on experimental observations. A thermally related equation is proposed to bridge the thermal creep coefficient with temperature. By incorporating the equation to a selected one-dimensional (1D) elastic viscoplastic (EVP) model, a thermal creep-based EVP model was developed which takes into account the influence of temperature on creep. Simulations of oedometer tests on reconstituted clay are made through coupled consolidation analysis. The bonding effect of the soil structure on compressive behavior for intact clay is studied. By incorporating the influence of the soil structure, the thermal creep EVP model is extended for intact clay. Experimental predictions for thermal creep oedometer tests are simulated at different temperatures and compared to that obtained from reconstituted clay. The results show that the influence of temperature on the creep behavior for intact clay is significant, and the model, this paper proposed, can successfully reproduce the thermal creep behavior of the soft clay under the 1D loading condition.

1. Introduction

It is well known that soft clays exhibit time-dependent behavior due to their viscosity. The long-term settlement of these clays after the dissipation of excess pore water pressure, which is sometimes called creep deformation, has been an important issue in geotechnical engineering. The creep behavior of the soft clay has been investigated experimentally in [1–5]. Based on that, some practical models have been developed [6–9].

Due to the deposition effect, interparticle bonds are usually formed in soft clays referred as the soil structure. When suffering loading for the soft clay, a significant progressive loss of bonds will happen. By comparing the compression curves in $e - \log\sigma_v^{'}$ (void ratio versus vertical effective stress in the log scale) for intact and reconstituted samples, the large differences observed are induced by the bond elimination. In addition, the bond elimination effect on the creep behavior of soft clays has been studied in [10, 11].

Soft clays are also subjected to the action of heat under many circumstances, for example, the nuclear waste isolation, heat energy storage, and geothermal development. Studies show that the creep behavior of soft clays is strongly related not only to the bonding structure but also to temperature. The creep behavior of these clays will be changed accordingly [12–16]. However, the effect of temperature on the creep behavior was somehow showed, but not well documented. It will be nice if there exists a direct way for modeling the thermal creep behavior.

For this purpose, we focus on the 1D behavior which can bring fundamental features for more mechanical behavior. Firstly, the temperature dependency behavior of creep is studied based on the experimental observations. Then, a thermally related EVP model for reconstituted clay is proposed by incorporating the effect of temperature.

Furthermore, the bonding elimination of the structure is incorporated into the thermal-based model. Finally, the prediction ability of the proposed model is shown by simulations at different conditions.

2. Temperature Dependency of Creep of Soil

2.1. Experimental Observations. The consolidation process of soil is usually divided into primary consolidation and secondary consolidation, and the boundary point is whether the excess pore pressure completely dissipates. Similarly, thermal secondary consolidation occurs for thermal consolidation after the dissipation of excess pore pressure [13]. Figure 1 shows an idealized thermal consolidation test result. Actually, thermal secondary consolidation occurs throughout the thermal consolidation process, and the induced deformation only relates to time and temperature. Thus, thermal creep used in this paper is more suitable for the process. The slope of the linear portion of the thermal consolidation curve is the thermal creep coefficient ψ_T, given in void ratio per log cycle.

A number of studies demonstrate that the temperature affects significantly the thermal creep coefficient. For example, Figure 2 presents the evolution of the thermal creep coefficient with increasing temperature for intact Pacific illite conducted by Houston et al. [13]. The values range from about 0.01 at 40°C to about 0.06 at 200°C. The increase in the rate of thermal creep deformation at the elevated temperatures was quite significant. Additionally, the creep-temperature tests on peats conducted by Fox and Edil [12] also show that creep dominates the consolidation process and temperature influences the creep rate significantly. Thus, it can be concluded that it is necessary to account for the effect of temperature on creep for soft intact clay.

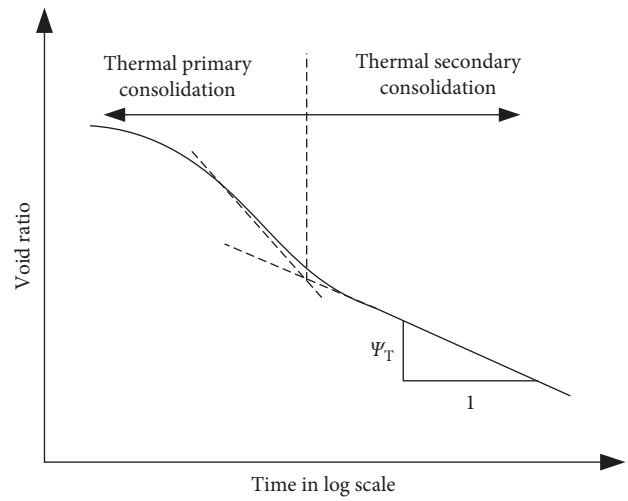

Figure 1: Definition of the thermal creep coefficient.

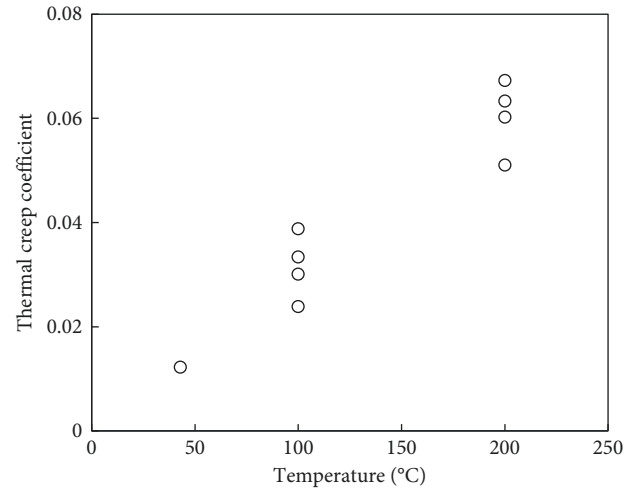

Figure 2: Evolution of the thermal creep coefficient of Pacific illite [13].

2.2. Proposed Thermal Creep Equation. Based on the experiments, different expressions were given to describe the temperature-dependent behavior of the thermal creep coefficient. The relationship between thermal creep coefficient and temperature can be linearly functioned by Houston et al. [13]. That is,

$$\psi_T = A \cdot T, \tag{1}$$

where ψ_T is the thermal creep coefficient under temperature T and A is the thermal relate parameter, which can be obtained by correlating the results as shown in Figure 2. Equation (1) describes ψ increasing linearly with temperature straightforwardly. However, we can observe that ψ_T will be zero when the temperature decreases to zero and ψ_T will be negative if the temperature still decreases and is unreasonable.

Based on the experimental results on peat, the following equation is used by Fox and Edil [12] to predict the value of ψ_T, due to a change in soil temperature:

$$\psi_T = \psi_{T_r} \exp\left[B\left(T - T_r\right)\right], \tag{2}$$

where ψ_{T_r} is the reference thermal creep coefficient under the reference temperature T_r, thermal relate parameter B is equal to 0.25 ± 0.02/°C for the peat in [12], and the parameter is independent of vertical effective stress and the magnitude of temperature change. Equation (2) describes that ψ increases nonlinearly with temperature. However, due to its mathematic structure, Equation (2) will deduce a very large number of ψ at a higher temperature, far beyond the normal range.

In this study, we propose a new equation to describe the nonlinear increase of the thermal creep coefficient with temperature, which can be written as

$$\psi_T = \psi_{T_r}\left(\frac{T}{T_r}\right)^{C_T}, \tag{3}$$

where C_T is the thermal relate parameter which can be correlated with the experiment results. This equation can overcome the deficiency exposed by Equations (1) and (2). Figure 3 plots the comparisons of the three equations

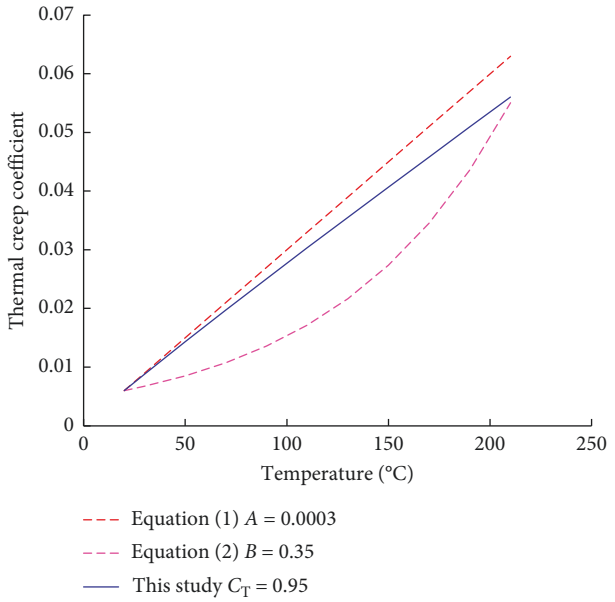

FIGURE 3: Comparisons of the equations describing the relationship between thermal creep coefficient and temperature.

describing the relationship between thermal creep coefficient and temperature. The point $T = 20^{\circ}\mathrm{C}$ and $\psi(20) = 0.006$ is adopted as the reference. As indicated, three equations give different shape curves. Overall, the curve plotted from Equation (3) is more practical than the others.

3. EVP Model considering the Temperature Effect on Creep

3.1. Adopted One-Dimensional Elastic Viscoplastic Model. First, a time-dependent stress-strain model without the thermal effect needs to be selected as a base [6]. The adopted model is presented briefly in this part.

Following the classic elastic viscoplastic approach, the total strain rate contains the elastic and viscoplastic strains rate, that is,

$$\dot{\varepsilon}_{\mathrm{v}} = \dot{\varepsilon}_{\mathrm{v}}^{\mathrm{e}} + \dot{\varepsilon}_{\mathrm{v}}^{\mathrm{vp}}, \tag{4}$$

where $\dot{\varepsilon}_{\mathrm{v}}$ represents the total strain rate and the superscripts "e" and "vp" denote the elastic and viscoplastic parts, respectively. The elastic strain rate is expressed as

$$\dot{\varepsilon}_{\mathrm{v}}^{\mathrm{e}} = \frac{\kappa}{1+e_0}\frac{\dot{\sigma}_{\mathrm{v}}'}{\sigma_{\mathrm{v}}'}, \tag{5}$$

where e_0 is the initial void ratio, σ_{v}' is the effective vertical stress, and κ is the slope of recompression lines in $e - \ln\sigma_{\mathrm{v}}'$ space.

For the viscoplastic strain rate, a one-dimensional formulation proposed by Kutter and Sathialingam [17] was adopted based on the creep coefficient ψ:

$$\dot{\varepsilon}_{\mathrm{v}}^{\mathrm{vp}} = \frac{\psi}{(1+e_0)\tau}\left(\frac{\sigma_{\mathrm{v}}'}{\sigma_{\mathrm{v}}'^{\mathrm{r}}}\right)^{\lambda-\kappa/\psi}, \tag{6}$$

where λ denotes the slope of the normal compression line in $e - \ln\sigma_{\mathrm{v}}'$ space; τ is the reference time, and it equals to the duration of each load increment in the oedometer test; and $\sigma_{\mathrm{v}}'^{\mathrm{r}}$ is the reference stress corresponding to the incremental time τ and increases with the development of the viscoplastic strain according to

$$\sigma_{\mathrm{v}}'^{\mathrm{r}} = \sigma_{\mathrm{p}}'^{\mathrm{r}}\exp\left(\frac{1+e_0}{\lambda-\kappa}\varepsilon_{\mathrm{v}}^{\mathrm{vp}}\right), \tag{7}$$

where $\sigma_{\mathrm{p}}'^{\mathrm{r}}$ denotes the preconsolidation pressure.

The above relationships have been suggested in [18–20] and validated in [6, 10].

3.2. Incorporation of the Thermal Effect. The effects of temperature on the stress-strain behavior of clay have been observed in the laboratory [12, 13], which are helpful to discuss the thermal effect on the parameters in the above constitutive model. Increase and decrease in temperature may produce changes in the bonding of clay particles and the viscosity of absorbed water. These changes alternately produce more or fewer changes in compressibility. However, the experiments conducted in [15, 21, 22] show that the variations of λ and κ with temperature are negligible. Furthermore, a volume change due to elastic expansion of the clay particle will occur during the drainage of thermal consolidation. Considering that the strain under a constant effective stress remains small [14, 23, 24] and the emphasis of this paper, the parameters λ, κ, and e_0 will remain constant when clays suffering a change of temperature.

The thermal creep coefficient can be incorporated into the basic EVP model directly. By substituting the parameter ψ in Equation (6) by Equation (3), the 1D thermal-related viscoplastic strain rate changes to

$$\dot{\varepsilon}_{\mathrm{v}}^{\mathrm{vp}} = \frac{\psi_{T_{\mathrm{r}}}}{(1+e_0)\tau}\left(\frac{T}{T_{\mathrm{r}}}\right)^{C_{\mathrm{T}}}\left(\frac{\sigma_{\mathrm{v}}'}{\sigma_{\mathrm{v}}'^{\mathrm{r}}}\right)^{\left((\lambda-\kappa)/\left(\psi_{T_{\mathrm{r}}}\right)\right)\left(T_{\mathrm{r}}/T\right)^{C_{\mathrm{T}}}}. \tag{8}$$

Actually, the preconsolidation pressure σ_{p}' also varies with temperature. The thermal-dependent behavior of σ_{p}' has been studied from the oedometer tests or isotropic compression tests with variable temperatures. All of the results indicate that σ_{p}' will decrease with an elevated temperature [25–29]. Based on the data collected from literature, Figure 4 plots the relationship between the normalized preconsolidation pressure and temperature. The regression analyses show that it is also reasonable to assume a linear relationship between $\log(\sigma_{\mathrm{p}}'/\sigma_{\mathrm{p}}'^{\mathrm{r}})$ and $\log(T/T_{\mathrm{r}})$, firstly proposed by [28]. Thus, the relationship between the preconsolidation pressure and temperature can be fitted by

$$\frac{\sigma_{\mathrm{p}}'}{\sigma_{\mathrm{p}}'^{\mathrm{r}}} = \left(\frac{T}{T_{\mathrm{r}}}\right)^{\theta}, \tag{9}$$

where θ is a thermal parameter and σ_{p}' and $\sigma_{\mathrm{p}}'^{\mathrm{r}}$ are the preconsolidation pressures at temperature T and the reference temperature T_{r}, respectively. The present model has no elastic limit, which is different from Perzyna's overstress method [30].

3.3. Coupled Consolidation Analysis. In the following numerical simulations of the conventional oedometer tests,

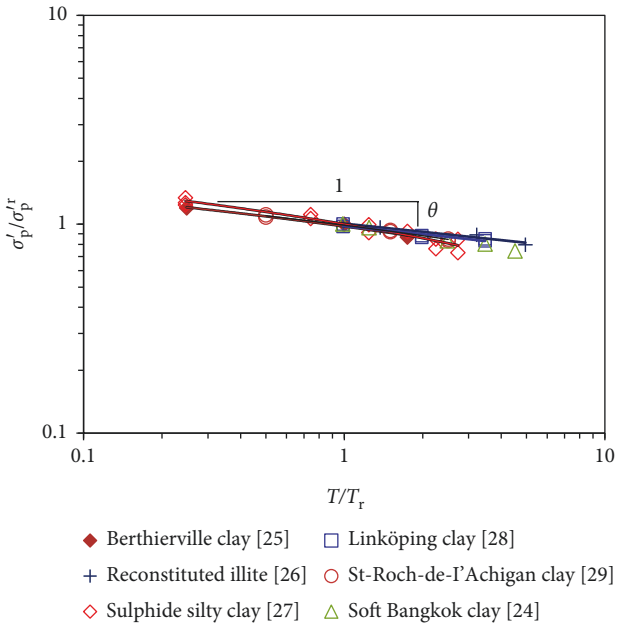

Figure 4: Temperature dependency of preconsolidation pressure.

soil-water coupling analysis will be performed. Darcy's law was adopted for the consolidation process:

$$-\frac{\partial \varepsilon_v}{\partial t} = \frac{1+e_0}{\gamma_w}\frac{\partial}{\partial z}\left(\frac{k}{1+e}\right)\frac{\partial u}{\partial z}, \tag{10}$$

where z is the vertical depth, u is the excess pore pressure, and k is the hydraulic conductivity. Actually, k is also influenced by temperature. A decrease in pore water viscosity will happen with increasing temperature, which will result in an increase in the permeability of the soil. Thus, increasing temperature will speed up the consolidation process. Considering the emphasis of this paper, only the void ratio-dependent behavior of k is considered, and according to experimental results, the evolution of k can be expressed as

$$k = k_0 10^{(e-e_0)/c_k}, \tag{11}$$

where the initial hydraulic conductivity k_0 is corresponding to e_0 and the permeability coefficient c_k can be easily measured from the oedometer test results by plotting $e - \log k$.

The above equations were implemented in finite element software PLAXIS Version 8, but in 1D, finite element simulations can be established for modeling the primary consolidation and the creep process in an oedometer test. Details of coupled consolidation and creep analysis can be found in [19, 31] and are not repeated here.

3.4. Simulated One-Dimensional Behavior. In order to validate the proposed thermal-dependent EVP model, numerical simulations for the assumed oedometer creep tests were performed at three temperatures (T = 20°C, 50°C, and 80°C). The results are shown in Figure 5, and the parameters adopted for these simulations are listed in Figure 5(a). The simulated temperature behavior agrees with the common experimental phenomena on unstructured clay, as expected by the model's principle. For example, the simulated relationship between the preconsolidation pressure and temperature corresponds to the input value of θ.

Take the simulated test on T = 80°C; for example, the compression behavior for each load increment is presented in Figure 5(b). The simulated thermal creep coefficient ψ = 0.013 agrees well with that obtained from Equation (3) with T_r = 20°C and ψ_{T_r} = 0.0065.

4. Thermal-Dependent EVP Model for Intact Clay

4.1. Bonding Effect on Compression Behavior. During the oedometer tests, the difference of the compression curves obtained on intact and reconstituted clay is caused by bonding elimination as shown in Figure 6(a) for Wenzhou clay [32]. The structures between soil particles for intact clay will be eliminated gradually during compressing. The tests conducted under variable temperatures show that the shape of the compression curves does not change with temperature, for instance, tests on intact Berthierville clay [25] and Linköping clay [28]. Thus, we assume that the process of bonding elimination is thermal independent but only relates to the strain level. Figure 6(b) presents the schematic plot of the stress-strain curve at an arbitrary temperature T for soft intact clay. For a given viscoplastic strain level ε_v^{vp}, the bond elimination results in the current stress σ'_v reaching point D for intact clay. Corresponding to the same viscoplastic strain, we define an intrinsic stress σ'_{vi} on the reconstituted sample. We assume that the difference between the current stress and intrinsic stress is due to the existing of the soil structure, based on which a bonding ratio $\chi = \sigma'_v/\sigma'_{vi} - 1$ can be proposed. Thus, the current stress σ'_v during straining can be expressed as

$$\sigma'_v = (1+\chi)\sigma'_{vi}. \tag{12}$$

Initially, the bonding ratio $\chi = \chi_0 = \sigma'_p/\sigma'_{pi} - 1$. Following the increasing of strain, the bonds are broken gradually and χ decreases from its initial value χ_0 ultimately towards zero when the bonds are completely eliminated as plotting in Figure 6(a). According to the definition, bonding ratio and the corresponding viscoplastic strain during compression is measured and plotted in Figure 6(c) for Wenzhou clay. Based on the results, we propose the following relationship to express the attenuation of bonding ratio:

$$\chi = \chi_0 e^{-\zeta \varepsilon_v^{vp}}, \tag{13}$$

where the parameter ζ controls the rate of bonding elimination (ζ = 8.0 for Wenzhou clay in Figure 6(c)). Actually, the intrinsic stress σ'_{vi} in Equation (12) can be regarded as the reference stress as indicated in Equation (8), and the bonding ratio can be regarded as the scaling parameter. Thus, the present model is then composed of Equations (8), (9), and (12). Combining with the elastic strain rate in Equation (5), the stress-strain curve for a given temperature can be obtained.

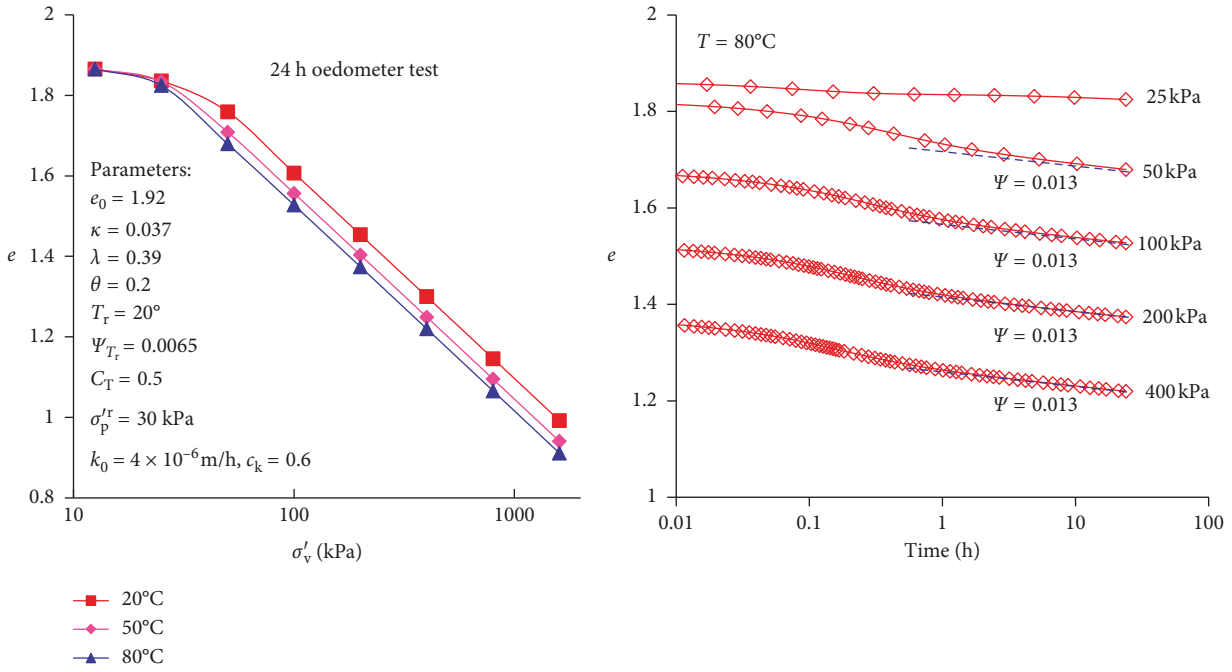

FIGURE 5: Simulations for 24 h oedometer tests: (a) compression curves at different temperatures; (b) compression behavior at each load increment for the test simulated at T = 80°C.

4.2. Model Parameters. The present model that combined creep and temperature involves a number of parameters which can be divided into four groups:

(a) Parameters related to compressibility: initial void ratio (e_0), the intrinsic slope of the compression line (λ_i), and the slope of the recompression line (κ). The values of λ_i and κ can be measured from the oedometer tests on the reconstituted and intact samples, respectively. As the thermal expansion and contraction are neglected in this paper, e_0 can be measured initially at the reference temperature.

(b) Parameter related to bonding elimination: the initial bonding ratio (χ_0) and the parameter ζ. The value of χ_0 can be measured from the oedometer tests on the intact and reconstituted samples conducted at the same temperature. It needs to point out that, for χ_0, high-quality intact samples are needed. The parameter ζ representing the bonding elimination rate can be derived from Equations (12) and (13):

$$\zeta = -\ln\left\{\frac{1}{\chi_0}\left[\frac{\sigma_v'}{\sigma_{vi}'} - 1\right]\right\}\frac{1}{\varepsilon_v^{vp}}, \tag{14}$$

where ε_v^{vp} is the volumetric viscoplastic strain corresponding to σ_v' (Figure 6(b)) at an arbitrary temperature. Thus, ζ can be calculated by selecting a point on the postyield curve.

(c) Parameters of creep: reference thermal creep coefficient (ψ_{T_r}) and thermal parameter (C_T). ψ_{T_r} can be measured directly from the oedometer tests on reconstituted at a reference temperature (T_r). C_T can be obtained by correlating ψ_{T_r} with temperature.

Parameters related to preconsolidation pressure: the reference preconsolidation pressure ($\sigma_p^{'r}$) at the reference temperature T_r and the thermal parameter (θ). $\sigma_p^{'r}$ can be obtained at the intersection of the compression curves for the reconstituted and intact samples, as shown in Figure 6(b). θ can be obtained directly from the oedometer tests on the reconstituted or intact samples at different temperatures. Wang et al. [33] investigated the value of θ for seven clays and summarized that θ varies from 0.125 to 0.194. Furthermore, θ can be obtained by the empirical correlation of liquid limit (w_L) expressed as

$$\theta = 0.1072 + 0.0008 w_L. \tag{15}$$

Thus, θ can be obtained by correlating without carrying out the temperature-controlled tests.

Thus, ten model parameters (e_0, κ, λ, θ, T_r, C_T, ψ_{T_r}, $\sigma_p^{'r}$, χ_0, and ζ) are required for the model, and all of the parameters can be determined straightforwardly from the temperature-controlled oedometer test.

5. Calibration and Validation

5.1. Predictions on Wenzhou Clay. The thermal creep coefficient ψ is also influenced by the bonding elimination process during straining. In order to evaluate the model ability to reproduce the behavior of soft intact clay, simulations were performed for the thermal oedometer tests with different temperatures. The input ordinary parameters are the same as those given in Table 1. For intact clay, two

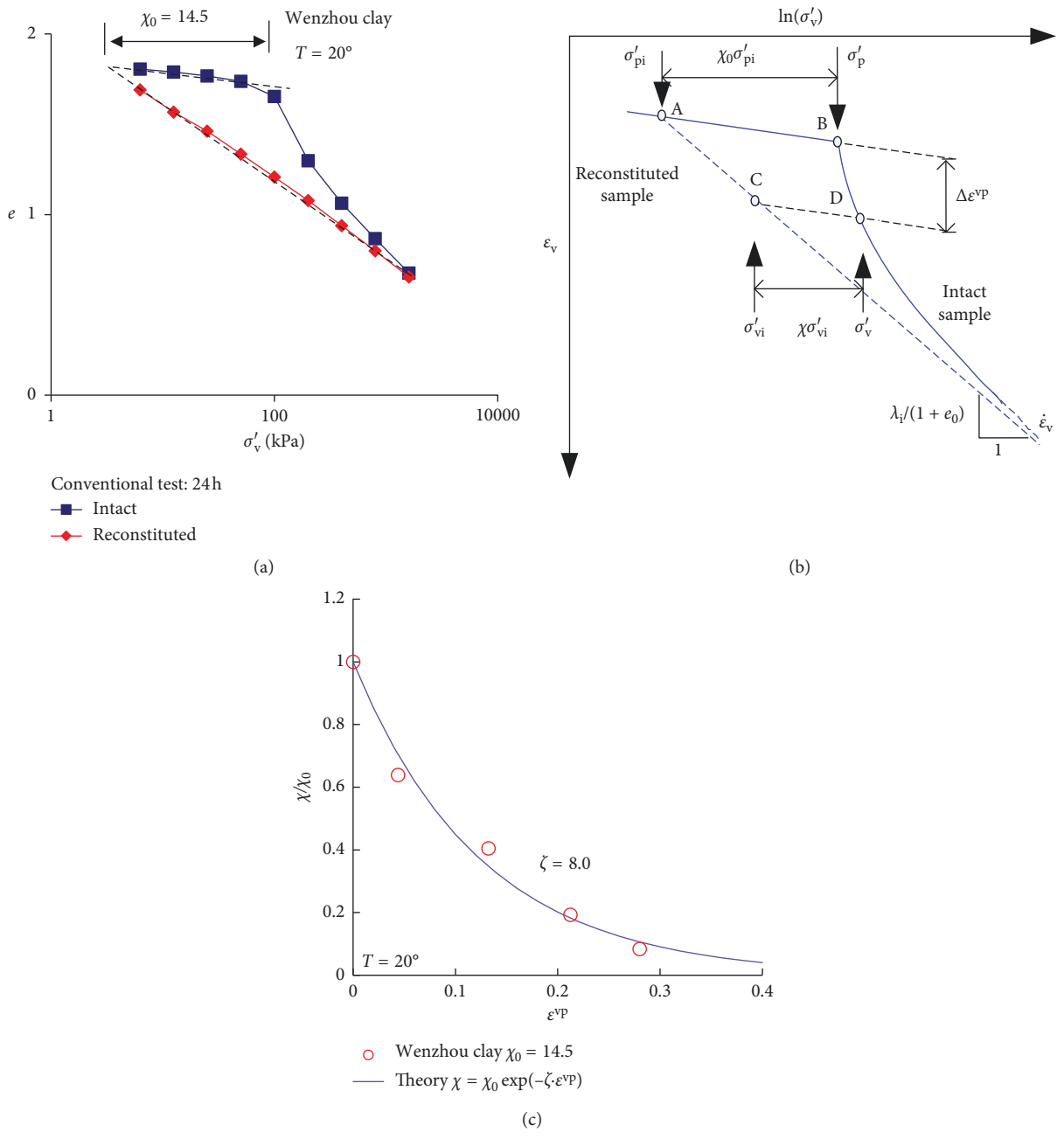

Figure 6: Bonding effect on the compressibility and the evolution of bonding ratio: (a) compression curves for intact and reconstituted Wenzhou clay at T =20°C; (b) illustration of the bonding elimination with viscoplastic strain; (c) evolution of bonding ratio with viscoplastic strain.

Table 1: Values of model parameters and state variables for selected clays.

clay	$\lambda\Lambda$	κ	e_0	σ'^{r}_p kPa	χ_0	ζ	θ	T_r	ψ_{T_r}	C_T	k (m/h)	c_k
Wenzhou	0.39	0.037	1.92	30	3.5	8	0.2	70	0.006	0.5	4×10^{-6}	0.6
Utby	0.18	0.03	1.98	55	54	15	0.15	20	0.02	0.31	2×10^{-6}	0.99
Tokyo bay	0.36	0.05	2.4	79	0.4	7	0.17	20	0.031	—	1×10^{-7}	1.2

parameters $\chi_0 = 3.5$ and $\zeta = 8$ were used. Three temperatures with $T = 20°C$, 50°C, and 80°C are adopted in the simulations.

Figure 7 shows typical results of the thermal oedometer tests in natural intact clay simulated by the new model:

(1) In Figure 7(a), the compression curves in different temperatures are similar to the oedometer test on intact Wenzhou clay (Figure 6(a)). The preconsolidation pressure is influenced significantly by

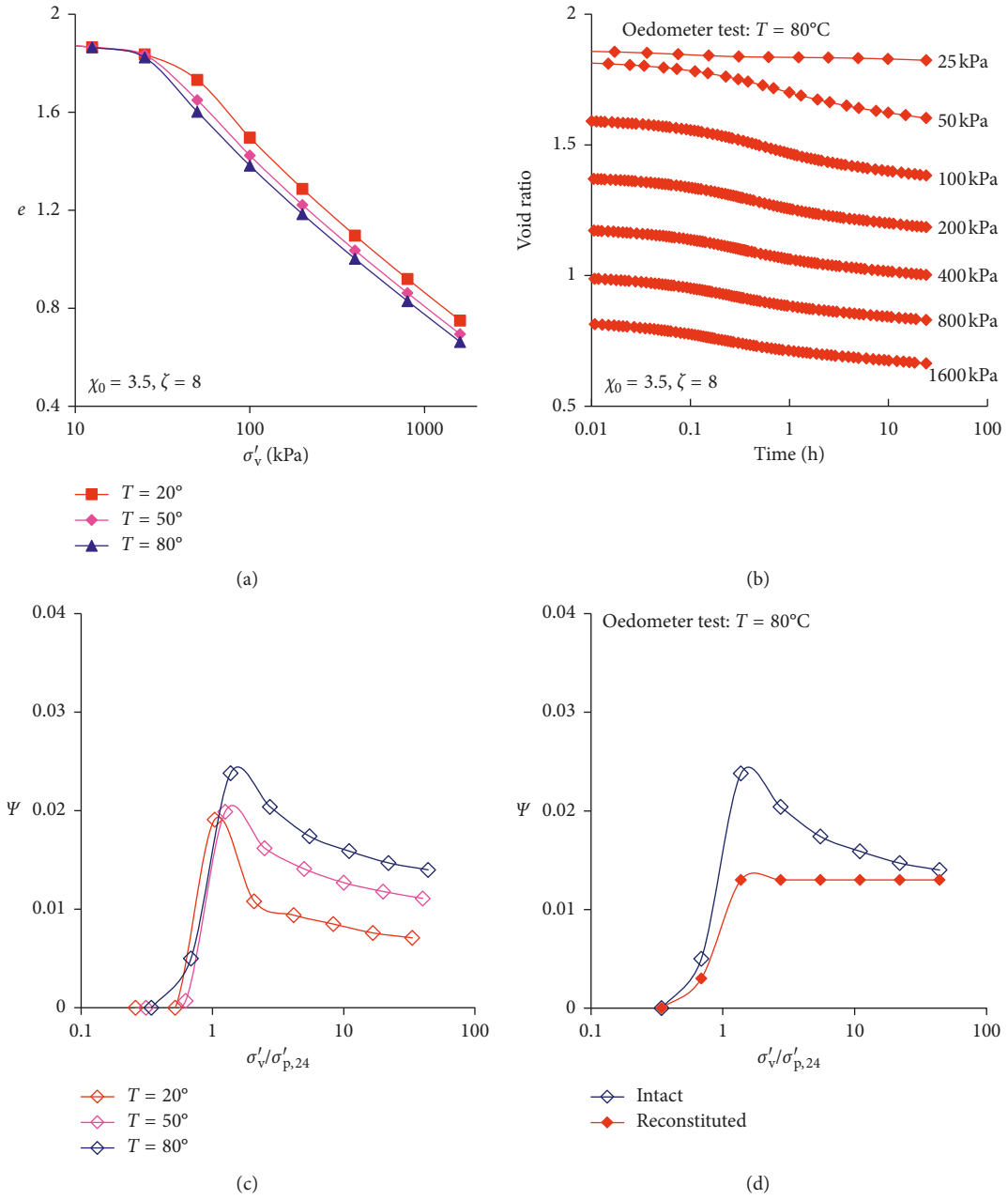

Figure 7: Predictions of the thermal oedometer test on Wenzhou clay with different temperatures: (a) compression curves at different temperatures; (b) strain-time curves for the case with $T = 80^{\circ}C$; (c) evolution of the thermal creep coefficient with normalized vertical stress; (d) comparisons of the thermal creep coefficient between intact and reconstituted clay.

the temperature as presented in Figure 5 on reconstituted clay.

(2) In Figure 7(b), the typical curves of strain versus time were reproduced for natural intact clay, where the thermal creep coefficient ψ can be obtained at the end of each load; here, only the simulation results for $T = 80^{\circ}C$ are presented.

(3) In Figure 7(c), the measured ψ at three temperatures were plotted versus the normalized applied stress by the preconsolidation pressure. Here, the preconsolidation pressure is different for the three tests. The value ψ for intact clay increases rapidly with the applied stress, and when the stress reaches the preconsolidation pressure, ψ reaches a peak value and then decreases. The difference between these curves is due to the combined influence of temperature and bonding elimination.

(4) In Figure 7(d), the measured ψ for intact and reconstituted clay are compared for the test at $T = 80^{\circ}C$. The difference between the two curves is due to the existence of bonding and its elimination.

5.2. Predictions on Utby Clay. Li et al. [34] presented a set of the long-term oedometer tests on Utby clay (6 m depth) with

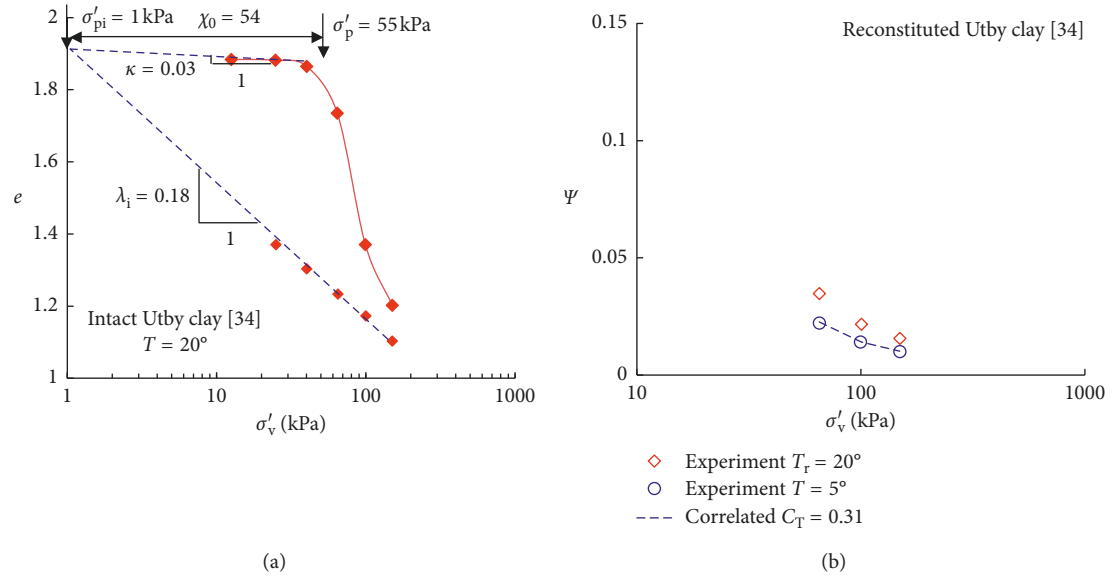

FIGURE 8: Determination of parameters from the thermal oedometer test: (a) compression parameters at T = 20°; (b) the thermal creep coefficient based on the experiment on the reconstituted sample.

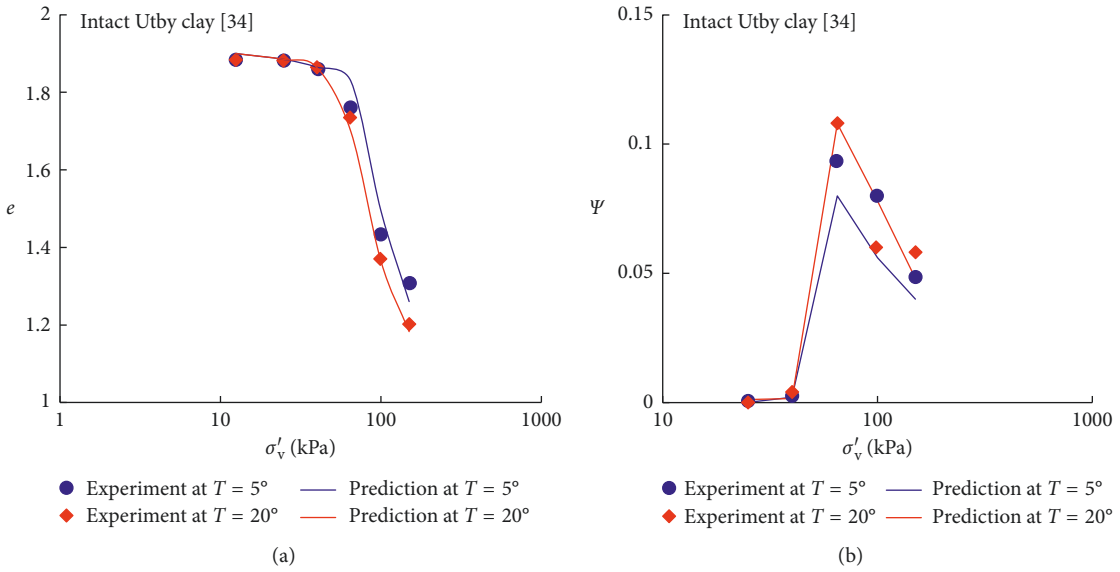

FIGURE 9: Predictions of the thermal oedometer test on intact Utby clay (depth = 6 m) with different temperatures: (a) compression curves; (b) creep coefficient.

different temperatures for both intact and reconstituted samples. The clay properties are as follows: liquid limit w = 55%, e_0 = 1.977, and σ'_p = 55 kPa for the intact sample at the reference room temperature T = 20°. The other parameters for the model were correlated with thermal oedometer tests results. Figure 8(a) shows the compression tests on intact and reconstituted samples at T_r = 20°. The parameter λ_i = 0.18 is determined based on the results of the reconstituted sample. The parameter κ =0.003 is correlated from the recompression curve. Bonding ratio χ_0 = 54 is obtained based on the method described above. The value of ζ = 15 was determined by selected a stress-strain point in Figure 8(a) and using Equation (14). Figure 8(b) presents the variation of the thermal creep coefficient with temperature. Adopting ψ_T at T = 20° as a reference, the predicted values of ψ_T for T=5° agree well with the experimental results with C_T = 0.31. Furthermore, an average value of ψ_{T_r} = 0.02 is used based on the experimental results at T = 20°. With Equation (15), θ = 0.15 is adopted in the simulation. To simulate the long-term creep test, the permeability of soil was taken as 4×10^{-6} m/h estimated from the consolidation curves of vertical strains versus time. The value of c_k was equal to $e_0/2$, as suggested by Tavenas et al. [35] based on observations on soft marine clays. All of the parameters are summarized in Table 1.

Figure 9 shows the comparison between experimental and simulation results. The predicted compression behavior

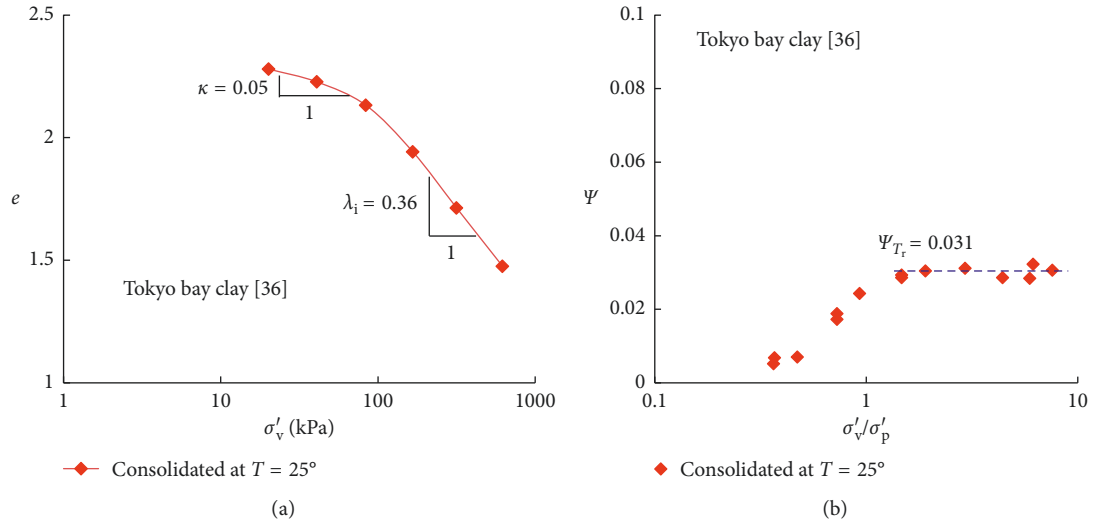

Figure 10: Determination of parameters from the oedometer tests for the sample consolidated at room temperature: (a) compression curves; (b) creep coefficient versus vertical stress.

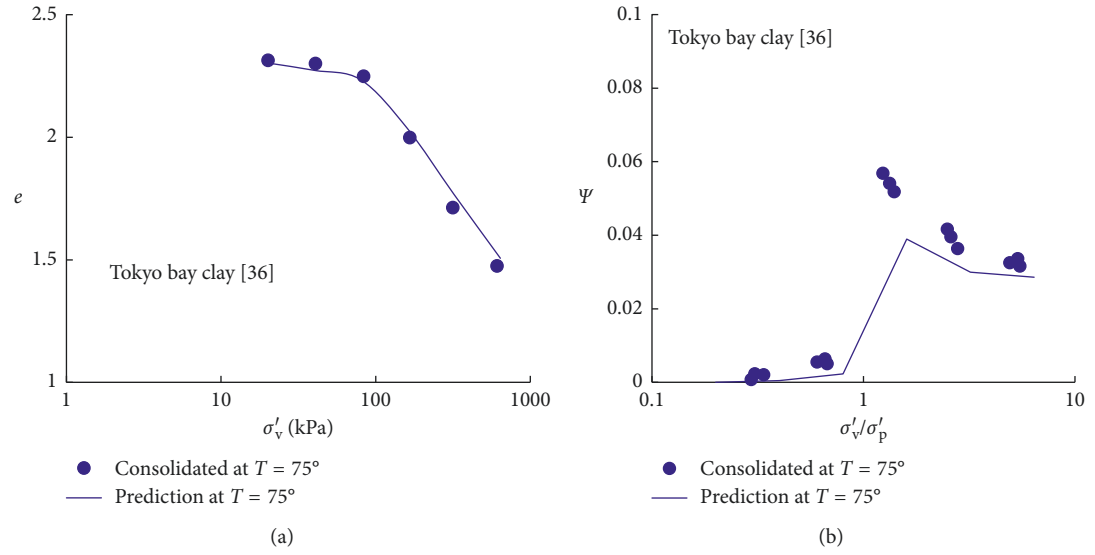

Figure 11: Predictions of the oedometer test on Tokyo bay clay consolidated at high temperatures: (a) compression curves; (b) creep coefficient versus normalized vertical stress.

at different temperatures shows good agreement with the experimental results for the values of the preconsolidation pressures and for the shape of the compression curves (Figure 9(a)). Furthermore, the predicted thermal creep coefficient also agrees well with the experimental results. For the values of vertical stress equal to the preconsolidation pressure, the thermal creep coefficient reaches to the maximum value (Figure 9(b)). It can be concluded that it is necessary to account for the coupling effect of temperature and destructuration for accurate predictions of the thermal compression behavior of the soft clay.

5.3. Predictions on Tokyo Bay Clay. Tsuchida et al. [36] conducted the oedometer tests on Tokyo bay clays which are consolidated at room temperature (25°) and at high temperature (75°), respectively. The sample which is suffered consolidating at a high temperature and cooled after the completion consolidation will behave like the lightly aged clay. Adopting the sample consolidated at room temperature as a reference, the properties are as follows: liquid limit w = 78% and e_0 = 2.4. From the experimental results on the sample consolidated at room temperature (Figure 10(a)), the parameter λ_i = 0.36, κ =0.05, and σ'_p = 79 kPa can be obtained. In addition, the reference ψ_{T_r} = 0031 is averaged for the vertical stress larger than preconsolidation pressure (Figure 10(b)). Also, the parameter θ = 0.17 can be calculated by Equation (15). χ_0 = 0.2 is obtained by the increase of preconsolidation pressure due to the cooling of the sample after high temperature consolidation. Similarly, ζ = 7 is

correlated based the compression curve, and the consolidation-related parameters $k = 1 \times 10^{-7}$ m/h, $c_k = 1.2$. All of the parameters are collected in Table 1.

Figure 11(a) shows that the predicted compressibility of Tokyo bay clay consolidated at a high temperature agrees well with the experiment. Furthermore, the predicted thermal creep coefficient has the same shape with experiment. The predicted values are a little smaller than the experimental results (Figure 11(b)). Overall speaking, the model can reproduce well the thermal creep behavior for the soft clay.

6. Conclusions

The temperature-dependent behavior of creep for soft intact clay has been investigated based on experimental observations from experimental results. A thermally related equation is proposed to bridge the thermal creep coefficient with temperature. By incorporating the equation to a selected one-dimensional EVP model, a thermal creep-based EVP model is developed taking into account the temperature dependency of creep. The determination of the model parameters is straightforward. Numerical simulations have been conducted to examine the predictive ability of the model for the soft clay.

Experimental predictions have carried out the thermal oedometer tests at different temperatures. The bonding elimination effect on the evolution of the thermal creep coefficient has been highlighted by comparing predictions with and without considering bonding elimination.

The results demonstrate that the proposed model can well reproduce temperature-dependent creep behavior of soft intact clay under the one-dimensional loading condition. Future work will be done to extend the proposed model to three-dimensional general stress space.

Data Availability

No data were used to support this study.

Conflicts of Interest

The authors declare that there are no conflicts of interests regarding the publication of this article.

Acknowledgments

We acknowledge with gratitude the financial support provided by the Fundamental Research Funds for the Central Universities (2015QNA64).

References

[1] G. Mesri and P. Godlewski, "Time and stress-compressibility interrelationship," *Journal of the Geotechnical Engineering Division*, vol. 103, no. 5, pp. 417–430, 1977.

[2] S. Leroueil, M. Kabbaj, F. Tavenas, and R. Bouchard, "Stress–strain–strain rate relation for the compressibility of sensitive natural clays," *Géotechnique*, vol. 35, no. 2, pp. 159–180, 1985.

[3] J. H. Yin, J. G. Zhu, and J. Graham, "A new elastic viscoplastic model for time-dependent behaviour of normally and overconsolidated clays: theory and verification," *Canadian Geotechnical Journal*, vol. 39, no. 1, pp. 157–173, 2002.

[4] Q. Y. Zhu, Z. Y. Yin, P. Y. Hicher, and S. L. Shen, "Nonlinearity of one-dimensional creep characteristics of soft clays," *Acta Geotechnica*, vol. 11, no. 4, pp. 887–900, 2016.

[5] Z. Y. Yin, M. Hattab, and P. Y. Hicher, "Multiscale modeling of a sensitive marine clay," *International Journal for Numerical and Analytical Methods in Geomechanics*, vol. 35, no. 15, pp. 1682–1702, 2011.

[6] Z. Y. Yin and J. H. Wang, "A one-dimensional strain-rate based model for soft structured clays," *Science China Technological Sciences*, vol. 55, no. 1, pp. 90–100, 2012.

[7] Z. Y. Yin, M. Karstunen, C. S. Chang, M. Koskinen, and M. Lojander, "Modeling time-dependent behavior of soft sensitive clay," *Journal of Geotechnical and Geoenvironmental Engineering*, vol. 137, no. 11, pp. 1103–1113, 2011.

[8] J. H. Yin and J. Graham, "Elastic visco-plastic modelling of one-dimensional consolidation," *Geotechnique*, vol. 46, no. 3, pp. 515–527, 1996.

[9] Z. Y. Yin, Q. Y. Zhu, J. H. Yin, and Q. Ni, "Stress relaxation coefficient and formulation for soft soils," *Géotechnique Letters*, vol. 4, no. 1, pp. 45–51, 2014.

[10] Q. Y. Zhu, Z. Y. Yin, D. M. Zhang, and H. W. Huang, "Numerical modeling of creep degradation of natural soft clays under one-dimensional condition," *KSCE Journal of Civil Engineering*, vol. 21, no. 5, pp. 1668–1678, 2017.

[11] Z.-Y. Yin, Q. Y. Zhu, and D. M. Zhang, "Comparison of two creep degradation modeling approaches for soft structured soils," *Acta Geotechnica*, vol. 12, no. 6, pp. 1395–1413, 2017.

[12] P. J. Fox and T. B. Edil, "Effects of stress and temperature on secondary compression of peat," *Canadian Geotechnical Journal*, vol. 33, no. 3, pp. 405–415, 1996.

[13] S. L. Houston, W. N. Houston, and N. D. Williams, "ThermoMechanical behavior of seafloor sediments," *Journal of Geotechnical Engineering*, vol. 111, no. 11, pp. 1249–1263, 1985.

[14] C. J. R. Coccia and J. S. McCartney, "Thermal volume change of poorly draining soils I: critical assessment of volume change mechanisms," *Computers and Geotechnics*, vol. 80, pp. 26–40, 2016.

[15] N. Jarad, O. Cuisinier, and F. Masrouri, "Effect of temperature and strain rate on the consolidation behaviour of compacted clayey soils," *European Journal of Environmental & Civil Engineering*, vol. 3, pp. 1–18, 2017.

[16] L. Laloui, S. Leroueil, and S. Chalindar, "Modelling the combined effect of strain rate and temperature on one-dimensional compression of soils," *Canadian Geotechnical Journal*, vol. 45, no. 12, pp. 1765–1777, 2008.

[17] B. L. Kutter and N. Sathialingam, "Elastic viscoplastic modelling of the rate-dependent behaviour of clays," *Géotechnique*, vol. 42, no. 3, pp. 427–441, 1992.

[18] P. A. Vermeer and H. P. Neher, "A soft soil model that accounts for creep," in *Proceedings of Plaxis Symposium Beyond 2000 in Computational Geotechnics*, Amsterdam, Netherlands, March 1999.

[19] D. F. E. Stolle, P. A. Vermeer, and P. G. Bonnier, "Time integration of a constitutive law for soft clays," *Communications in Numerical Methods in Engineering*, vol. 15, no. 8, pp. 603–609, 1999.

[20] M. Leoni, M. Karstunen, and P. A. Vermeer, "Anisotropic creep model for soft soils," *Géotechnique*, vol. 58, no. 3, pp. 215–226, 2008.

[21] R. G. Campanella and J. K. Mitchell, "Influence of temperature variation on soil behavior," *Journal of Soil Mechanics and Foundation Division*, vol. 94, pp. 609–734, 1968.
[22] A. Tsutsumi and H. Tanaka, "Combined effects of strain rate and temperature on consolidation behavior of clayey soils," *Soils and Foundations*, vol. 52, no. 2, pp. 207–215, 2012.
[23] C. Cekerevac and L. Laloui, "Experimental study of thermal effects on the mechanical behaviour of a clay," *International Journal for Numerical and Analytical Methods in Geomechanics*, vol. 28, no. 3, pp. 209–228, 2004.
[24] H. M. Abuel-Naga, D. T. Bergado, A. Bouazza, and G. V. Ramana, "Volume change behaviour of saturated clays under drained heating conditions: experimental results and constitutive modeling," *Canadian Geotechnical Journal*, vol. 44, no. 8, pp. 942–956, 2007.
[25] M. Boudali, S. Leroueil, and B. R. Srinivasa Murthy, "Viscous behaviour of natural clays," in *Proceedings of the 13th International Conference on Soil Mechanics and Foundation Engineering*, pp. 411–416, A. A. Balkema, Rotterdam, Netherlands, 1994.
[26] N. Tanaka, "Thermal elastic plastic behaviour and modelling of saturated clays," Doctoral thesis, University of Manitoba, Winnipeg, Manitoba, Canada, 1995.
[27] L. G. Eriksson, "Temperature effects on consolidation properties of sulfide clays," in *Proceedings of the 12th International Conference on Soil Mechanics and Foundation Engineering*, pp. 2084–2090, A. A. Balkema, Rotterdam, Netherlands, 1989.
[28] L. Moritz, "Geotechnical properties of clay at elevated temperatures," Report: 47, Swedish Geotechnical Institute, Linköping, Sweden, 1995.
[29] M. E. S. Marques and S. Leroueil, "Viscous behaviour of St-Roch-de-l'Achigan clay, Quebec," *Canadian Geotechnical Journal*, vol. 41, no. 1, pp. 25–38, 2004.
[30] P. Perzyna, "Fundamental problems in viscoplasticity," *Advances in Applied Mechanics*, vol. 9, no. 2, pp. 243–377, 1966.
[31] Y. Kim and S. Leroueil, "Modeling the viscoplastic behaviour of clays during consolidation: application to Berthierville clay in both laboratory and field conditions," *Canadian Geotechnical Journal*, vol. 38, no. 3, pp. 484–797, 2001.
[32] L. L. Zeng, Z. S. Hong, S. Y. Liu et al., "Variation law and quantitative evaluation of secondary consolidation behavior for remolded clays," *Chinese Journal of Geotechnical and Engineering*, vol. 34, no. 8, pp. 1496–1500, 2012.
[33] L. Z. Wang, K. J. Wang, and Y. Hong, "Modeling temperature-dependent behavior of soft clay," *Journal of Engineering Mechanics*, vol. 142, no. 8, article 04016054, 2016.
[34] Y. L. Li, J. Dijkstra, and M. Karstunen, "Thermomechanical creep in sensitive clays," *Journal of Geotechnical and Geoenvironmental Engineering*, vol. 144, no. 11, article 04018085, 2018.
[35] F. Tavenas, P. Leblond, and S. Leroueil, "The permeability of natural soft clay, part II. permeability characteristics," *Canadian Geotechnical Journal*, vol. 20, no. 4, pp. 645–660, 1983.
[36] A. Tsutsumi and H. Tanaka, "Combined effects of strain rate and temperature on consolidation behavior of clayey soils," *Soils and Foundations*, vol. 52, no. 2, pp. 207–215, 2012.